Reactions of Laser-Ablated Mo and W Atoms with Dinitrogen: Infrared Spectra of Metal Nitrides, Dinitrides, and Complexes in Solid Argon and Nitrogen

Lester Andrews,* Philip F. Souter,† William D. Bare, and Binyong Liang

Department of Chemistry, University of Virginia, Charlottesville, Virginia 22901

Received: February 16, 1999; In Final Form: March 23, 1999

Laser-ablated Mo and W atoms react with N_2 in excess nitrogen and argon to form the metal nitrides, MN, and ligated complexes, $(NN)_xMN$, the metal dinitrides, NMN, and ligated complexes, $(NN)_xMN_2$, and several complexes $M(NN)_x$ leading up to the octahedral species with $x = 6$. On the basis of the resolution of natural abundance Mo isotopes and ^{15}N substitution, the open, bent NMoN molecule valence angle is $106 \pm 3°$. The dinitride molecules are formed both by direct insertion of metastable metal atoms into dinitrogen and by the addition of atomic nitrogen to the mononitride molecule.

Introduction

Dinitrogen fixation is well-known in biochemical systems, and this process takes place in the molybdenum−iron nitrogenase cofactor (MoFe) with transition metal binding sites.[1−6] There have been hundreds of different transition metal−dinitrogen complexes characterized, each exhibiting different dinitrogen bond reduction.[4,7−10] For example, the catalytic conversion of dinitrogen into silylamines using molybdenum and tungsten dinitrogen complexes has been demonstrated.[8] Calculations have suggested that W(III) complexes may cleave dinitrogen better than Mo(III) complexes.[11]

In addition, dinitrogen reacts with molybdenum and tungsten surfaces at high temperature to give metal nitride films, which have found numerous applications as catalysts and electronic devices.[12−17] It is significant that dinitrogen dissociatively chemisorbs on W(100) surfaces.[18] However, kinetic studies showed no reactivity between ground-state Mo and N_2 in the gas phase,[19] but thermal Mo atoms condensed at 14 K with high (5−95%) N_2 concentrations in Kr revealed new product absorptions.[20] It is significant that laser-ablated Mo atoms in a low-pressure N_2 atmosphere form MoN.[21,22] Hence, an effective way to prepare Mo and W nitrides for matrix infrared investigation is to react the laser-ablated metal atoms with dinitrogen.

Molybdenum nitride is the most thoroughly studied second-row transition metal nitride; the rotational constant, vibrational frequency, and dipole moment are known.[21−29] In addition, electronic, infrared, and ESR spectra have been observed in matrix isolation experiments, and the $^4\Sigma^-$ ground state confirmed.[30,31] On the other hand, only the $A^4\Pi \rightarrow X^4\Sigma^-$ emission spectrum for WN has been reported in the gas phase.[32] However, a large number of X−W≡N complexes provide complementary information on WN species.[33] The analogous CrN molecule has been investigated; theoretical calculations, gas-phase emission, and matrix vibrational spectra have been reported.[34−36] In addition, a bent N−Cr−N dinitride molecule was characterized in the matrix work, and isotopic substitution at both atomic positions provided a $109 \pm 3°$ measurement of the valence angle.[36] Very recent calculations have suggested that several dinitride states are possible for the Mo and W systems.[37,38] Here follows an investigation of laser-ablated Mo and W atom reactions with N_2 and matrix infrared spectra of the metal nitrides, dinitrides, and complexes.

Experimental Section

The laser-ablation and matrix infrared experiments have been described previously.[39,40] The 1064 nm Nd:YAG laser beam (Spectra Physics, DCR-11) was focused by a 10 cm f.l. lens onto the rotating metal target (Mo, Goodfellow, 99% and W, Johnson-Matthey, 99.99%). The laser repetition rate is 10 Hz, and the pulse width is 10 ns. Laser powers ranging from 20 to 40 mJ/pulse at the sample were used in these experiments. The ablated metal atoms were codeposited with 1−4% N_2 in argon or pure nitrogen onto a 7 K CsI window at a rate of 2−4 mmol/h for 1−2 h. Natural isotopic nitrogen (Matheson, bone dry), $^{15}N_2$, mixtures, and scrambled $^{14,15}N_2$ (Isotec) were used. FTIR spectra were recorded with 0.5 cm^{-1} resolution and 0.1 cm^{-1} accuracy on a Nicolet 750 instrument. Matrix samples were annealed at different temperatures, and selected samples were subjected to broadband photolysis by a medium-pressure mercury arc lamp (Phillips, 175 W) with globe removed.

Calculations

Density functional theory (DFT) calculations using the Gaussian 94 program[41] were employed to estimate structural parameters and frequencies for MN and MN_2 to provide support for vibrational assignments. The BP86 functional, D95* basis set for nitrogen, and Los Alamos ECP plus DZ basis set for metal atoms were used for all calculations.[42−44]

Results

Laser-ablated Mo and W atoms react with N_2 in nitrogen and excess argon gas to produce new product absorptions, which are listed in Tables 1−5. Observations for $^{15}N_2$ and isotopic mixtures are also given. Figures 1−7 illustrate important regions of the spectra, which will be described below with the assignments to new molecules. Table 6 summarizes DFT calculations for metal nitride and dinitride states relevant to the experimental observations.

* Corresponding author. E-mail: lsa@virginia.edu.

† Current address: Procter and Gamble Corp., Newcastle-on-Tyne, England.

10.1021/jp990572+ CCC: $18.00
Published on Web 05/26/1999

TABLE 1: Absorptions (cm^{-1}) Observed for Laser-Ablated Mo Codeposited with Pure Dinitrogen

$^{14}N_2$	$^{15}N_2$	$^{14}N_2 + {}^{15}N_2$	scrambled $^{14,15}N_2$	R(14/15)	assign
2327.5	2249.8	doublet	triplet	1.03454	N_2
2317.6	2240.4	doublet	triplet	1.03446	$X-N_2$
2218.5	2144.6			1.03646	?
2178.1	2105.6			1.03443	$Mo(NN)_x$
2149.5	2078.1			1.03436	$(NN)_xMo(N_2)$
2132	2061			1.03444	$(NN)_xMoN$
2113.9	2043.8	sextet	strong triplet	1.03430	$Mo(NN)_6$
2055.9	1987.5			1.03442	$Mo(NN)_x$
2031.3	1963.8				$Mo(NN)_x$
1968.1	1902.7	1937.8	1937.8, 1934.7	1.03437	$Mo(NN)_2$
1935.3	1871			1.03437	MoNN ?
1914.1	1850.6			1.03431	MoNN ?
1816.9	1756.8	1816.9, 1756.8	1816.9, 1786.2, 1756.8	1.03421	$(NN)_xMo(N_2)$
1710.6	1653.8		1711, 1683, −	1.03435	$Mo(N_2)$?
1032.9	1002.5			1.03032	$(NN)_x{}^{92}MoN$
1029.0	998.5			1.03054	$(NN)_x{}^{98}MoN$
1027.7	997.3	doublet	doublet	1.03048	$(NN)_xMoN$
1026.4	996.0			1.03052	$(NN)_xMoN$
975.1	945.4	triplet	triplet	1.03142	$(NN)_x{}^{98}MoN_2$
935.6	908.1			1.03028	broad
865.8	841.5	triplet	triplet	1.02888	$(NN)_x{}^{92}MoN_2$
864.8	840.5	triplet	triplet	1.02891	$(NN)_x{}^{92}MoN_2$
861.6	837.2	triplet	triplet	1.02914	$(NN)_x{}^{98}MoN_2$
860.6	836.2	triplet	triplet	1.02918	$(NN)_x{}^{98}MoN_2$
833.2	809			1.02991	broad
771.9	746.8			1.03361	broad
668.6	649.4			1.02954	$(MoN)_2$?
657.5	638.9			1.02911	$(MoN)_2$?
520.5	508.5	sextet	514.3	1.02360	$Mo(NN)_6$
506.5	493.6			1.02613	$Mo(NN)_x$
478.6	462.4			1.03503	$Mo(NN)_x$
460.7	445.9	459, 447.4	459.3, 453.2, 446.7	1.03319	$Mo(NN)_x$

TABLE 2: Absorptions (cm^{-1}) Resolved for Natural Isotopic Abundance Mo Reacting with Pure $^{14}N_2$ and $^{15}N_2$[a]

Mo	$^{14}N_2$	$^{15}N_2$
92	865.80	841.50
94	864.36	840.01
95	863.64	839.28
96	862.95	838.58
97	862.27	837.86
98	861.61	837.20
100	860.34	835.87

[a] Resolution 0.1 cm^{-1}, frequency accuracy ±0.03 cm^{-1}.

TABLE 3: Absorptions (cm^{-1}) for Laser-Ablated Mo Co-deposited with N_2 in Excess Argon

$^{14}N_2$	anneal	$^{15}N_2$	$^{14}N_2 + {}^{15}N_2$	R(14/15)	assign
2146.6	0, +	2075.7	broad	1.03416	$(NN)_xMoN$
2123.9	0, +	2053.4	broad	1.03433	$Mo(NN)_6$?
2070.6	+, −	2002.0	broad	1.03427	$Mo(NN)_x$
2029.1	+, −	1961.4	broad	1.03452	$Mo(NN)_x$
1997.8	+, −	1930.3	broad triplet	1.03497	$Mo(NN)_x$
1964.8	+, −	1899.5	broad doublet	1.03438	$Mo(NN)_2$?
1938.7	0, −	1874.1	doublet	1.03441	MoNN ?
1055.2	+, −	1024.5	doublet	1.02988	MoN site
1051.0	+, −	1020.2	doublet	1.03019	^{98}MoN site
1041.4	−, −	1011.1	doublet	1.02997	MoN site
1037.5	−, −	1008.0	doublet	1.02927	^{98}MoN
1028.9	+, +	997.9	doublet	1.03107	$(NN)_xMoN$
1014.0	−, −	984.2	doublet	1.03082	?
1009.3	−, −	979.7	doublet	1.03021	?
881.5	−, −	856.8	doublet	1.02883	$^{92}MoN_2$
879.3	−, −	854.6	doublet	1.02890	site
877.1	−, −	852.4	doublet	1.02898	$^{98}MoN_2$
861.2	+, +	836.9	triplet	1.02904	?
598.2	+, +	580.2	broad	1.03102	?
589.9	+, +	572.3	broad	1.02867	
491.5	+, +	477.8	broad	1.02867	
482.8	+, +	468.7	broad	1.03008	

Discussion

Molybdenum and tungsten mononitrides and dinitrides and dinitrogen complexes will be identified from matrix infrared spectra with isotopic substitution.

MoN. Molybdenum nitride is the most studied second-row transition metal nitride. The observed gas-phase vibrational frequencies for the most abundant $^{98}Mo^{14}N$ and lightest $^{92}Mo^{14}N$ isotopic molecules are 1044.7 and 1049.6 cm^{-1}, respectively.[28] The matrix spectra are in excellent agreement; we can only resolve the most abundant $^{98}Mo^{14}N$ isotopic molecule in the major red matrix site at 1037.5 cm^{-1} in solid argon. A minor blue matrix site reveals this band at 1051 cm^{-1} (Figure 1). These observations are in agreement with a previous 1040 cm^{-1} argon matrix assignment to MoN.[30] The $^{98}Mo^{14}N/^{98}Mo^{15}N$ ratio, 1.02916, for the major site is slightly lower than the calculated harmonic diatomic values 1.03051 owing to anharmonicity in the observed vibrational potentials.

Annealing the argon matrix decreased the red and blue sites and produced a new feature at 1028.9 cm^{-1}, which was the only absorption in this region to survive 40 K annealing. Photolysis, however, decreased the red in favor of the blue site absorption. The nitrogen matrix revealed a similar 1029 cm^{-1} band that increased with structure at 1032.9, 1029.0, 1027.7, and 1026.4 cm^{-1} on annealing to 20 K (Figure 2) that appears to be due to molybdenum isotopes and sites. The $Mo^{15}N$ counterparts give isotopic ratios of 1.0305, which are nearer the harmonic MoN value. Photolysis decreased this band in favor of a 1035 cm^{-1} feature, but annealing to 30 K restored most of the structured 1029 cm^{-1} band and destroyed the 1035 cm^{-1} band. In the upper region, a 2132 cm^{-1} absorption tracked with the 1029 cm^{-1} absorption on photolysis and annealing including blue sites for both.

The 1037.5 cm^{-1} absorption is assigned to $^{98}Mo^{14}N$ in solid argon, a 7.2 cm^{-1} red shift from the gas-phase fundamental for

TABLE 4: Absorptions (cm^{-1}) Observed for Laser-Ablated W Atom Reactions with Pure Dinitrogen

$^{14}N_2$	$^{15}N_2$	R(14/15)	assign
2466.4	2385.0	1.03413	$W(NN)_6$ combo
2327.4	2249.7	1.03454	N_2
2288.1	2211.6	1.03459	?
2250.1	2175.2	1.03443	?
2183.8	2111.3	1.03434	?
2154.1[b]	2082.5	1.03438	$W(NN)_x$
2147.9	2076.5	1.03438	$(NN)_xW(N_2)$
2143.2	2071.9	1.03441	$(NN)_xW(N_2)$
2122	2051	1.03462	$(NN)_xWN$
2087.7[a]	2018.1	1.03449	$W(NN)_6$
2055[b]	1986	1.03474	$W(NN)_x$
2005.1[b]	1938.5	1.03436	$W(NN)_x$
1944.5[a]	1879.7	1.03447	$W(NN)_x$
1886.1[a]	1824.2	1.03393	$W(NN)_x$
1871.0[c]	1809.4	1.03404	$(NN)_xW(N_2)$
1863.9[c]	1802.5	1.03406	$(NN)_xW(N_2)$
1747.3[b]	1689.3	1.03433	$W(N_2)$?
1037.0	1004.6	1.03225	$(NN)_xWN$
1027.9	995.7	1.03234	$(NN)_xWN$
990.5	959.6	1.03220	$(NN)_xWN$
988.9	957.8	1.03247	$(NN)_xWN$
950.2	920.4	1.03238	$(NN)_xW_mN_n$
906.7	877.1	1.03377	$(NN)_xW_mN_n$
876.4	849.4	1.03179	$(NN)_xWN_2$
870.3	863.7	1.03152	$(NN)_xWN_2$
865.1	836.6	1.03216	$(NN)_xWN_2$
857.3	830.6	1.03216	$(NN)_xWN_2$
814.3	787.4	1.03416	$(NN)_xW_mN_n$
762.5	738.7	1.03222	broad
744.3	721.4	1.03174	broad
523.0[a]	507.3	1.03095	$W(NN)_6$
450.5	436.0	1.03326	$W(NN)_x$

[a] Bands increased on stepwise annealing. [b] Bands increased then decreased on stepwise annealing. [c] Bands produced on annealing, destroyed by photolysis, and increased on further annealing.

TABLE 5: Absorptions (cm^{-1}) Observed for Laser-Ablated W Atom Reactions with N_2 in Excess Argon

$^{14}N_2$	$^{15}N_2$	R(14/15)	assign
2160	2088	1.03448	?
2135.1	2064.0	1.03440	$(NN)_xWN$
2093	2033	1.03460	$W(NN)_6$
2056.3	1988.0	1.03436	$W(NN)_x$
2044.9	1977.0	1.03434	$W(NN)_x$
2001.3	1934.6	1.03448	$W(NN)_x$
1981.7	1916.0	1.03429	$W(NN)_x$
1953.5	1889.0	1.03436	$W(NN)_x$
1894.3	1831.0	1.03457	WNN ?
1886.8	1824.4	1.03420	WNN site
1059.5	1026.5	1.03215	WN
1057.2	1024.2	1.03222	$(NN)_xWN$
1039.2	1007.0	1.03227	$(NN)_xWN$
1036.6	1004.3	1.03216	$(NN)_xWN$
1028.6	996.4	1.03232	$(NN)_xWN$
1024.5 sh	992.4 sh	1.03235	site
907.3	903.2	1.00454	NWO
882.1	878.7	1.00398	$(NN)_x$(NWO)
878.3	851.5	1.03147	WN_2
869.6	843.0	1.03155	$(NN)_xWN_2$
480.1	464.8	1.03292	$W(NN)_x$

the ground $^4\Sigma^-$ state molecule. This is in accord with DFT frequency calculations of a 1090 cm^{-1} harmonic fundamental, which must be scaled by 0.95 to fit the observed frequency.[45] The 2132 and 1029 cm^{-1} absorptions are assigned to the $(NN)_xMoN$ ligated complex with x most likely 5, where the 2132 cm^{-1} band is the dinitrogen ligand stretching mode. Ligation has a smaller effect on the MoN fundamental than in the CrN and VN cases.[36]

MoN_2. The sharp 877.1 cm^{-1} argon matrix band exhibits a lower 14/15 ratio, 1.02898, than the ^{98}MoN diatomic molecule, 1.03051, and it gives way on annealing to a band at 861.2 cm^{-1}, which also exhibits a low 14/15 ratio, 1.02904. The yield in solid nitrogen is much larger, and this major band is split into two sites at 861.6 and 860.6 cm^{-1} with 14/15 ratios of 1.02914 and 1.02918. Furthermore, counterparts for seven naturally occurring molybdenum isotopes (Figure 3) are observed with the natural abundance population, which demonstrates the participation of a single Mo atom. Table 2 gives the upper site band for each ^{n}Mo isotope; the lower site band is 1.0 cm^{-1} lower. In pure dinitrogen, these Mo isotopic absorptions give 1/2/1 triplet patterns with $^{14}N_2 + {}^{15}N_2$ and scrambled $^{14,15}N_2$ reagents indicating that the product contains two equivalent N atoms and that it is formed by sequential reactions of N atoms from two different dinitrogen molecules. In solid argon, the 877.1 cm^{-1} band is assigned to ν_3 of the open N$-^{98}$Mo$-$N dinitride molecule (hereafter MoN_2 for convenience) and the 861.2 cm^{-1} band that appeared on annealing to the coordinatively saturated $(NN)_x{}^{98}MoN_2$ species that is produced in high yield at 861.6, 860.6 cm^{-1} in pure dinitrogen. With $^{14}N_2 + {}^{15}N_2$ in argon, the 871.1 cm^{-1} band and its 852.4 cm^{-1} $^{15}N_2$ counterpart exhibited *no* intermediate mixed isotopic component. This means that a single dinitrogen molecule is involved in the initial deposition reaction to form isolated N$-$Mo$-$N. However, on annealing, the 861.2 cm^{-1} $(NN)_xMoN_2$ band and its $^{15}N_2$ counterpart at 836.9 cm^{-1} exhibited a weaker 847.6 cm^{-1} mixed isotopic component (50% of 861.2 and 836.9 cm^{-1} bands), which shows that on annealing some $(NN)_xMoN_2$ is made by nitrogen atom reaction with the mononitride product.

The weaker 975.1 cm^{-1} band in pure dinitrogen tracks with the stronger 860.6 cm^{-1} band on annealing and on photolysis. This weaker band exhibits a slightly larger 14/15 ratio (1.03142) and a triplet in $^{14}N_2 + {}^{15}N_2$ and $^{14,15}N_2$ experiments, which is appropriate for the ν_1 mode of the ligated $(NN)_xMoN_2$ species. Furthermore, the common origin of the 975.1 and 860.6 cm^{-1} bands is demonstrated by matching asymmetries in their intermediate $^{14}N^{98}Mo^{15}N$ components at 961.6 and 846.7 cm^{-1}, which are respectively 1.3 cm^{-1} *higher* and 1.6 cm^{-1} *lower* than the averages of $^{98}Mo^{14}N_2$ and $^{98}Mo^{15}N_2$ values owing to interaction between these two bond-stretching modes in the mixed isotopic molecule of reduced symmetry.

The isotopic data (seven Mo isotopes and two N isotopes) in two matrix sites provide a basis for calculation of the N$-$Mo$-$N valence angle using apex and terminal atom isotopic substitution, which produce upper and lower limits to the valence angle owing to differences in anharmonicity.[40,46] The seven upper limits for the blue site range 108.6$-$109.2°, with 108.9° average and 0.2° standard deviation and for the red site range 108.3$-$108.9°, with 108.6° average and the same standard deviation. Lower limits were calculated for Mo isotopic mass pairs differing by 2 or more mass units. For the blue site, 17 lower limits range 101.8$-$104.1°, with 103.0° average and 0.5° standard deviation, and for the red site range 102.5$-$103.5°, with 103.0° average and 0.3° standard deviation. Hence, the NMoN valence angle is accurately determined as 106 ± 3° for the $(NN)_xMoN_2$ species in solid nitrogen. For MoN_2 isolated in solid argon, four data points for $^{98}Mo^{14}N_2$, $^{92}Mo^{14}N_2$, $^{98}Mo^{15}N_2$, and $^{92}Mo^{15}N_2$ gave 105 ± 1° lower and 111 ± 1° upper limits and a 108 ± 3° average valence angle. Hence, ligation by N_2 has no measurable effect on the N$-$Mo$-$N valence angle.

Similar calculations have been reported for MoO_2 with a comparable number of isotopic frequencies, and 125 ± 1° upper and 119 ± 3° lower limits were determined.[40] In the present 30

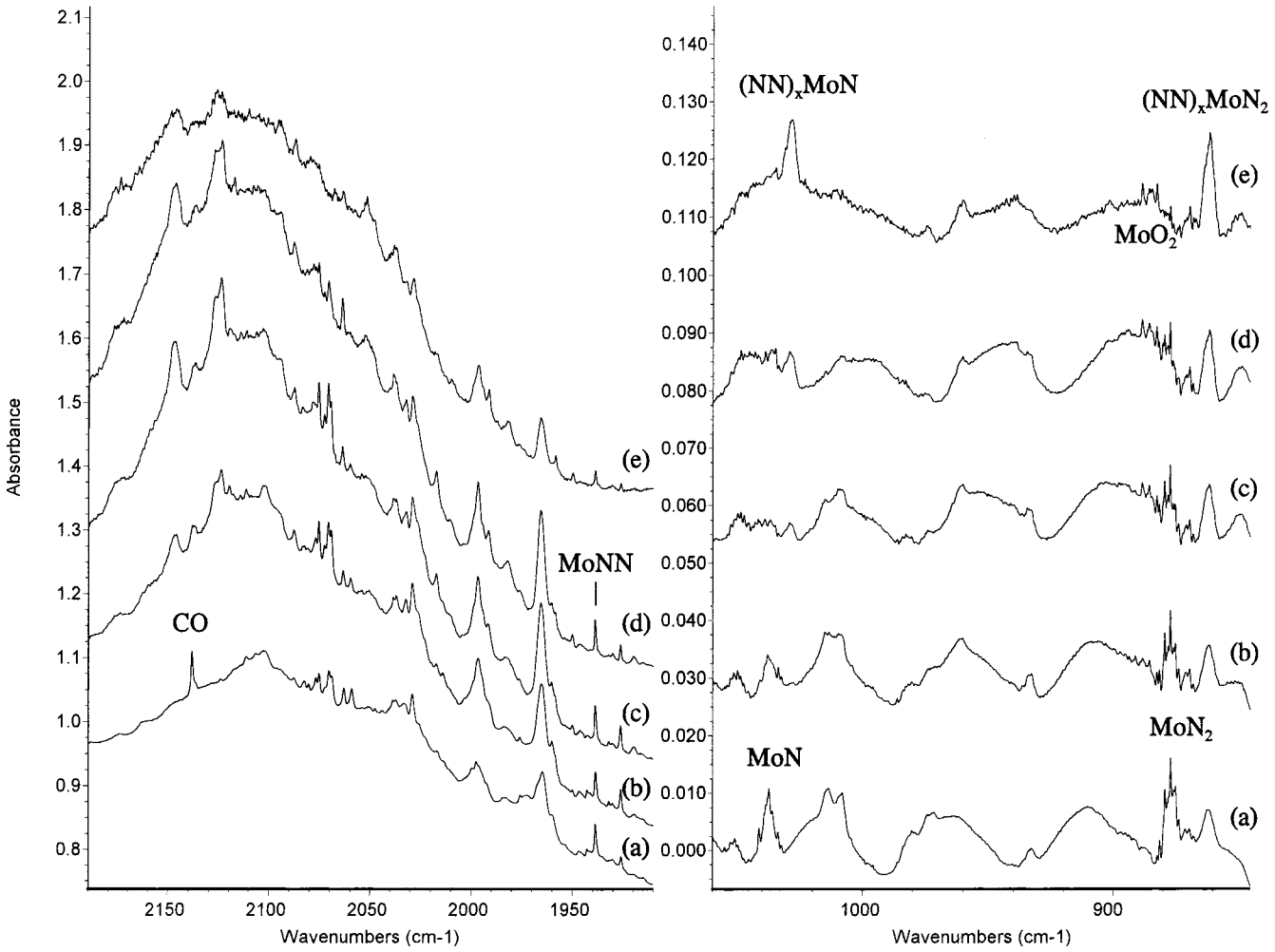

Figure 1. Infrared spectra in the 2190−1910 and 1060−845 cm^{-1} regions for laser-ablated Mo atoms codeposited with 2% N_2 in argon: (a) sample codeposited at 10 K for 2 h; (b) after annealing to 25 K; (c) after annealing to 30 K; (d) after annealing to 35 K; (e) after annealing to 40 K.

K annealing 0.1 cm^{-1} resolution spectrum, very sharp, weak MoO_2 impurity absorptions appeared 4.1 cm^{-1} to the red of site 1 in solid argon.[40] For the O−Mo−O valence angle, 17 lower limits in solid nitrogen range 125.5−126.7° and average 126.0° with 0.3° standard deviation. In the case of MoO_2, ligation by N_2 may slightly open the valence angle (by up to 7°).

A number of different isomers of MoN_2 and WN_2 have been predicted by theoretical calculations, and the energy ordering is very sensitive to the theoretical method employed.[37,38] There are two stable NMoN structures, a cyclic form and an open, bent form. Energetic laser-ablated Mo atoms are able to produce the open, bent N−Mo−N structure, which has frequencies and a bond angle near those for one of the structures described by theory. First, the Salahub group found the $^5\Pi$ MoNN and $^5B_1$ $Mo(N_2)$ complexes to be −3.5 and −1.7 kcal/mol, respectively, with respect to ground-state $Mo(^7S) + N_2$, and the $^1A_1$ and $^3B_2$ open, bent dinitrides to be +6.3 and +11.1 kcal/mol at the GGA level of DFT.[37] Second, the Pyykko group predicted these MoN_2 species to be +21.2, +16.3, +25.3, and +20.0 kcal/mol, respectively, above the ground-state atoms at the CASPT2 level of theory.[38] Since we have found BP86 frequencies to be a useful guide for Mo and W oxide assignments,[40] similar calculations were performed for the nitrides. Structures and frequencies for the $^1A_1$ and $^3B_2$ open, bent dinitrides calculated at the BP86 level are in reasonable agreement with previous calculations,[38] and the $^1A_1$ state is higher by 2.2 kcal/mol. The observed ν_3 and ν_1 fundamentals for NMoN (861.6 and 975.1 cm^{-1}) and valence angle (106 ± 3°) are compatible with the $^1A_1$ state parameters calculated by BP86 and by CCSD(T) methods.[38] These $^1A_1$ state BP86 frequencies, scaled by 0.922 and 0.930, fit the observed values, which are near the 0.95 scale factor required for MoN but lower than scale factors for the LanL effective core potential.[45] Furthermore, the calculated intensities are in the correct order, although the b_2 mode is 10 times and not 100 times stronger than the a_1 mode. However, the calculated $^3B_2$ state frequencies have the opposite relative intensity and the b_2 mode is calculated 10% *lower* than the observed value, which is not in the direction expected for the BP86 functional.[45] In addition, the CCSD(T) calculations[38] describe the same bent $^1A_1$ state and give stretching frequencies (1025 and 896 cm^{-1}) and valence angle (104.4°) in excellent agreement with the present DFT/BP86 values. Although calculations suggest that the open $^3B_2$ state is slightly lower than the $^1A_1$ state, the energy difference is within error in the calculations. It is significant that the dipole moment of the $^1A_1$ MoN_2 state (5.70 D) is substantially larger than that for the $^3B_2$ state (3.89 D), and the $^1A_1$ state will be preferentially stabilized by the matrix.

WN. In the W samples with N_2 in excess argon, a sharp, weak band at 1059.5 cm^{-1} gives way on annealing to a second band at 1057.2 cm^{-1}, then features at 1039.2 and 1036.6 cm^{-1}, and finally the absorption at 1028.6 cm^{-1} dominates after 40 K annealing. The spectra from a similar $^{15}N_2$ experiment (Figure 4) show the evolution of ^{15}N counterparts and define ratios ranging from 1.03215 to 1.03227 (Table 5), which are just below

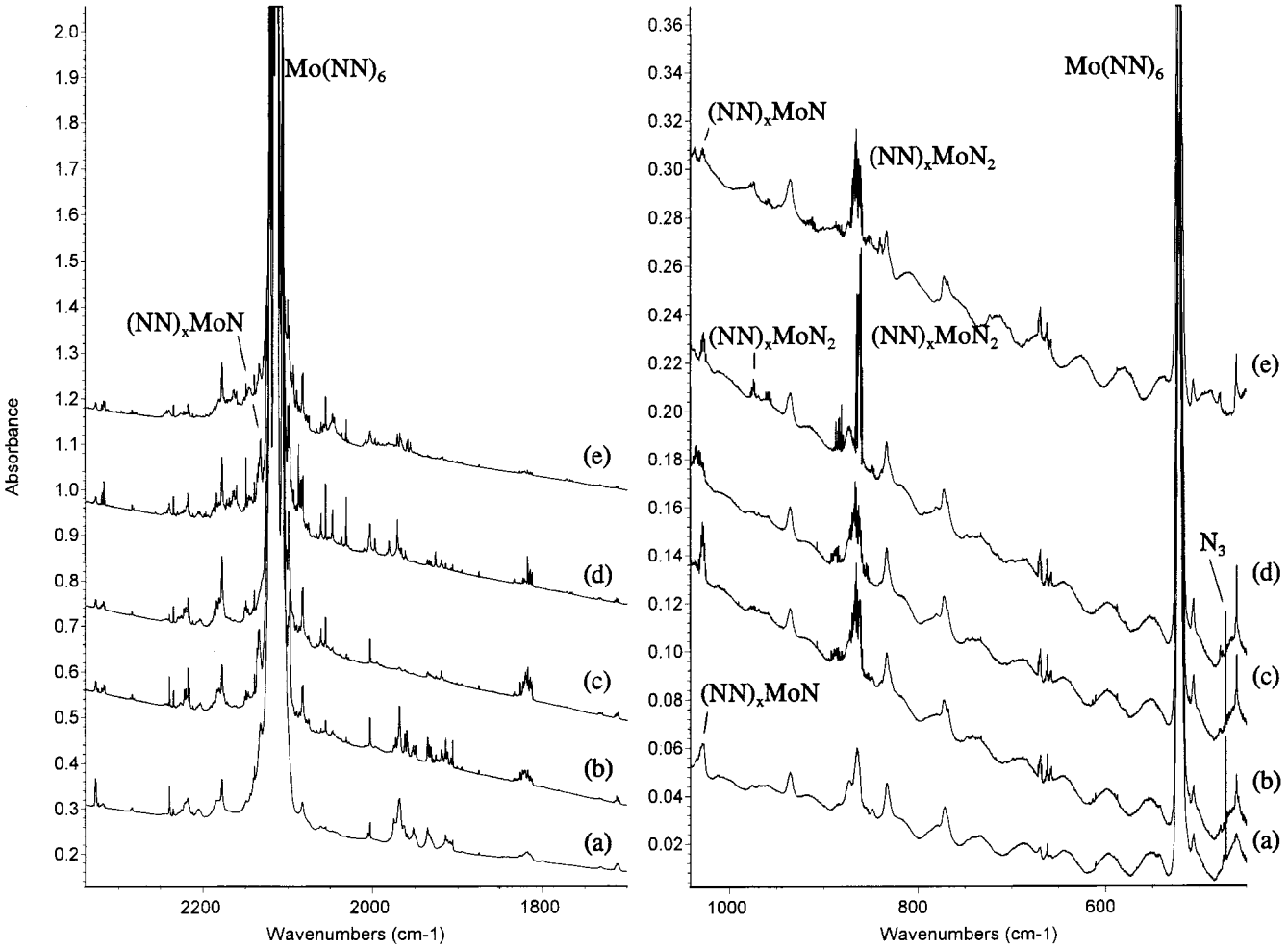

Figure 2. Infrared spectra in the 2340−1700 and 1050−450 cm^{-1} regions for laser-ablated Mo atoms codeposited with pure dinitrogen: (a) sample codeposited at 10 K for 1 h; (b) after annealing to 20 K; (c) after broadband photolysis for 20 min; (d) after annealing to 30 K; (e) after annealing to 35 K.

the harmonic diatomic WN ratio (1.03248). Spectra from a scrambled $^{14,15}N_2$ experiment (Figure 5) show no mixed isotopic components and demonstrate that a single N atom participates in this vibrational mode. In pure nitrogen, a strong 1027.9 cm^{-1} band with 1037.0 cm^{-1} satellite dominates this region (Figure 6); annealing to 20 K increases the former by 10% and decreases the latter, and higher annealing decreases both absorptions while a 988.9 cm^{-1} feature increases.

The sharp 1059.5 cm^{-1} band is assigned to WN isolated in solid argon. The DFT calculations predict a 1089 cm^{-1} harmonic fundamental for the ground $^4\Sigma^-$ state and a 1.678 Å bond length in excellent agreement with the gas-phase value (1.667 Å) from rotational analysis.[32] The 0.972 scale factor required to fit the DFT harmonic frequency to the argon matrix absorption is in the range of expected values.[45] The 1057.2, 1039.3, 1036.6, and 1028.6 cm^{-1} bands are due to $(NN)_xWN$ complexes formed by stepwise annealing and association of dinitrogen ligands. Note agreement between the major annealing band in argon (1028.6 cm^{-1}) and the strong band in pure dinitrogen (1027.9 cm^{-1}) for the saturated $(NN)_xWN$ complex. Finally, a weak 988.9 cm^{-1} band increases steadily on stepwise annealing until it dominates the 1027 cm^{-1} band after 35 K annealing (Figure 6). The 988.9 cm^{-1} band shows the same contour and isotopic behavior as the 1027.9 cm^{-1} band and is believed to arise from a more extensively ligated $(NN)_xWN$ species.

The observation of sharp, weak 1059.8 and 1026.8 cm^{-1} bands in ^{14}NO and ^{15}NO experiments[47] without the associated $(NN)_xWN$ bands (Table 5) provides support for the present matrix identification of WN. On the basis of earlier gas-phase and matrix observations, the gas-phase WN fundamental is predicted at 1070 ± 10 cm^{-1}.

It is interesting to compare the effect of ligation by N_2 on the CrN, MoN, and WN stretching frequencies. The 30.1 cm^{-1} displacement found[36] for CrN is in agreement with the 30.9 cm^{-1} value found for WN, but the MoN displacement on ligation is much smaller, 8.6 cm^{-1} if the 1037.5 cm^{-1} band is isolated MoN, but 22.2 cm^{-1} if measured from the weaker 1051.1 cm^{-1} blue site band. We note that ligation displaces VN and NbN lower by comparable 28.4 and 27.1 cm^{-1} values.[36,48] Finally, the lower $(NN)_xWN$ band at 988.9 cm^{-1} is displaced a much larger 70.6 cm^{-1} from isolated WN, much more in line with the ligand displacement found for NdN (853.3 − 782.0 = 71.3 cm^{-1}).[49]

The metal nitrides are produced here by the union of metal and nitrogen atoms during sample condensation where N atoms arise from dissociation of N_2 by impact with energetic laser-ablated metal atoms.[49−51] The formation of atomic nitrogen in these experiments is confirmed by the observation of N_3 radical at 1657.5 and 472.1 cm^{-1} in the pure dinitrogen investigations.[39,52]

$$M(Mo, W) + N \rightarrow MN \quad (1)$$

$$M(Mo, W) + N + xN_2 \rightarrow (NN)_xMN \quad (2)$$

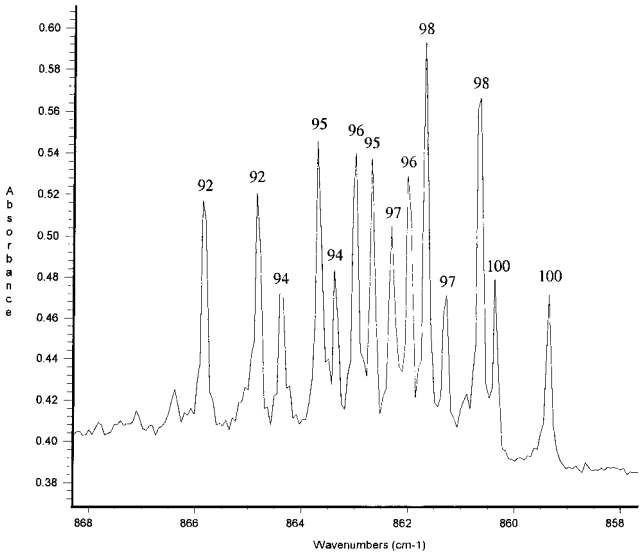

Figure 3. Infrared spectra in 868−858 cm^{-1} region recorded at 0.1 cm^{-1} resolution for Mo/N_2 sample from Figure 2d with ^{n}Mo isotopes indicated.

WN_2. In W samples with N_2 in excess argon, a sharp 878.3 cm^{-1} band decreases on annealing and a broader 869.6 cm^{-1} band increases (Figure 4). The 878.3 and 869.6 cm^{-1} bands form doublets using $^{14}N_2 + {}^{15}N_2$ with weak 863.5 and 854.8 cm^{-1} intermediate components, which can be described as 1/0.5/1 "triplets" (Figure 7). With statistical $^{14,15}N_2$, both bands form 1/2/1 triplets with intermediate components at 863.3 and 854.6 cm^{-1} (Figure 5). These bands exhibit smaller 14/15 ratios than the WN diatomic molecule, indicating more metal participation. In the pure dinitrogen matrix, the sharp 870.3 and 865.1 cm^{-1} bands increase on annealing and behave similarly on isotopic substitution; triplets are observed for both bands with isotopic mixtures, although the $^{14}N_2 + {}^{15}N_2$ experiment (Figure 7) gave intermediate components (855.4, 851.2 cm^{-1}) of comparable intensity to the 870.3, 865.1 cm^{-1} bands and the pure statistical $^{14,15}N_2$ experiment gave 1/2/1 triplets.

The 1/2/1 triplets with $^{14,15}N_2$ clearly show that the new molecule absorbing here contains two equivalent N atoms. Following the analogous behavior for the Mo species absorbing at 860 cm^{-1} (Figure 3), which clearly involves a single Mo atom, these absorptions are assigned to the open, bent N−W−N dinitride molecule, called WN_2 for convenience. These species have different degrees of dinitrogen ligation with 878.3 cm^{-1} presumably due to isolated WN_2 in solid argon and 869.6 cm^{-1} to the generic complex $(NN)_xWN_2$.

The 14/15 isotopic ratios provide data for calculation of the N−W−N valence angle upper limit. The argon matrix bands give 113° and 111°, while the nitrogen matrix bands produce 112° and 110°. These values may be compared with the upper limits for MoN_2 (109°) and CrN_2 (113°),[36] from which it can be concluded that these bent dinitride molecules have about the same valence angle (105−110°).

Identification of the open, bent NWN species is also supported by electronic structure calculations.[38] Although the $^1A_1$ state is calculated here to be higher than the $^3B_2$ state, the b_2 frequency and angle fit the observed values better, and the higher calculated dipole moment again suggests that the $^1A_1$ state will be stabilized more by the matrix. Furthermore, the calculations suggest that the $^1A_1$ state has substantial W≡N triple bond character. Finally, we expect the analogous situation for NCrN, namely a bent $^1A_1$ state is trapped in the solid nitrogen matrix.

The bent NWN molecule with substantial triple bond character is in contrast to linear NUN.[53,54] The low-symmetry structure of NWN (C_{2v}) is in excellent agreement with the low symmetry (trigonal prismatic, D_{3h}, *not* octahedral) of two similar tungsten compounds, WH_6 from calculations[55] and $W(CH_3)_6$ from experiment.[56]

The mixed $^{14}N_2 + {}^{15}N_2$ isotopic argon matrix experiments show that most of the initial NMoN and NWN product molecules are formed by insertion of laser-ablated metal atoms, presumably in the metastable excited state, into a single dinitrogen molecule, reaction 3. The weak mixed isotopic absorption indicates that some dinitride is formed by the addition of N atoms to the mononitride, reaction 4. This process also occurs for the ligated species, reaction 5, and is the source of CrN_2 in the Cr/N_2 experiments,[36] and some of the MoN_2 and WN_2 in pure dinitrogen. There is no evidence for reaction 3 with cold metal atoms.

$$M^*(Mo, W) + N_2 \rightarrow N-M-N \quad (3)$$

$$N + MN\ (Mo, W) \rightarrow N-M-N \quad (4)$$

$$N + (NN)_xMN \rightarrow (NN)_xMN_2 \quad (5)$$

Preliminary thermal W atom experiments with pure dinitrogen (Klotzbücher, W. E., unpublished) showed the strong band at 2088 cm^{-1} to be assigned to $W(NN)_6$, without any of the bands assigned here to nitrides.

Higher Nitride Clusters. The broad bands at 950.2, 906.7, and 814.3 cm^{-1} in the nitride stretching region for W in pure N_2 decrease slightly on annealing and exhibit 14/15 ratios, which *increase* from the W−N diatomic value to almost that for a pure N motion (Table 4). This suggests that tungsten clusters W_m with increasing m may be involved. The pure $^{14}N_2 + {}^{15}N_2$ experiment gave broad bands extending between the pure $^{14}N_2$ and pure $^{15}N_2$ frequencies, which shows that three or more N atoms are required. These bands are clearly due to higher nitride clusters $(NN)_xW_mN_n$. Although the precise stoichiometry cannot be determined, the band absorbances (Figure 6) clearly demonstrate the great reactivity of tungsten for nitrogen, as shown by dissociative chemisorption.[18] Similar broad bands at 935.6, 833.2, and 771.9 cm^{-1} for Mo in pure N_2 (Figure 2) exhibit the same behavior and can be associated with analogous species. It is interesting to note that molybdenum and tungsten clusters form complexes with N_2 in the gas phase,[57,58] and that cluster size affects the binding of molecular as opposed to atomic nitrogen, i.e., the formation of species described here as nitrides.

Dinitrogen Complexes. Following the characterization of $Cr(NN)_6$ by very strong 2112.6 cm^{-1} stretching and strong 548.5 cm^{-1} deformation modes,[36] the 2113.9 and 520.5 cm^{-1} bands are assigned to $Mo(NN)_6$, and the 2087.7 and 523.0 cm^{-1} absorptions to $W(NN)_6$ all in solid nitrogen. As for Cr, the $^{14}N_2 + {}^{15}N_2$ spectra provide the diagnostic information. For Mo, the very strong 2113.9 and 2043.8 cm^{-1} bands bracket weaker intermediate 2076.9, 2066.6, 2060 sh, 2057.6 cm^{-1} absorptions for the antisymmetric N−N stretching mode with weaker 2205.4, 2196.8, 2187.8, 2177.0, and 2163.0 cm^{-1} bands for the symmetric N−N stretching modes of lower symmetry mixed isotopic molecules. For W, the very strong 2087.7 and 2018.1 cm^{-1} bands bracket sharp 2064.5, 2052.1, 2042.3, and 2038.8 cm^{-1} intermediate features for the antisymmetric N−N motion with weaker 2188.1, 2179.6, 2170.1, 2159.1, and 2144.9 cm^{-1} bands for the symmetric N−N modes of mixed isotopic molecules. The 14/15 ratio for the very strong $^{14}N_2$ and $^{15}N_2$

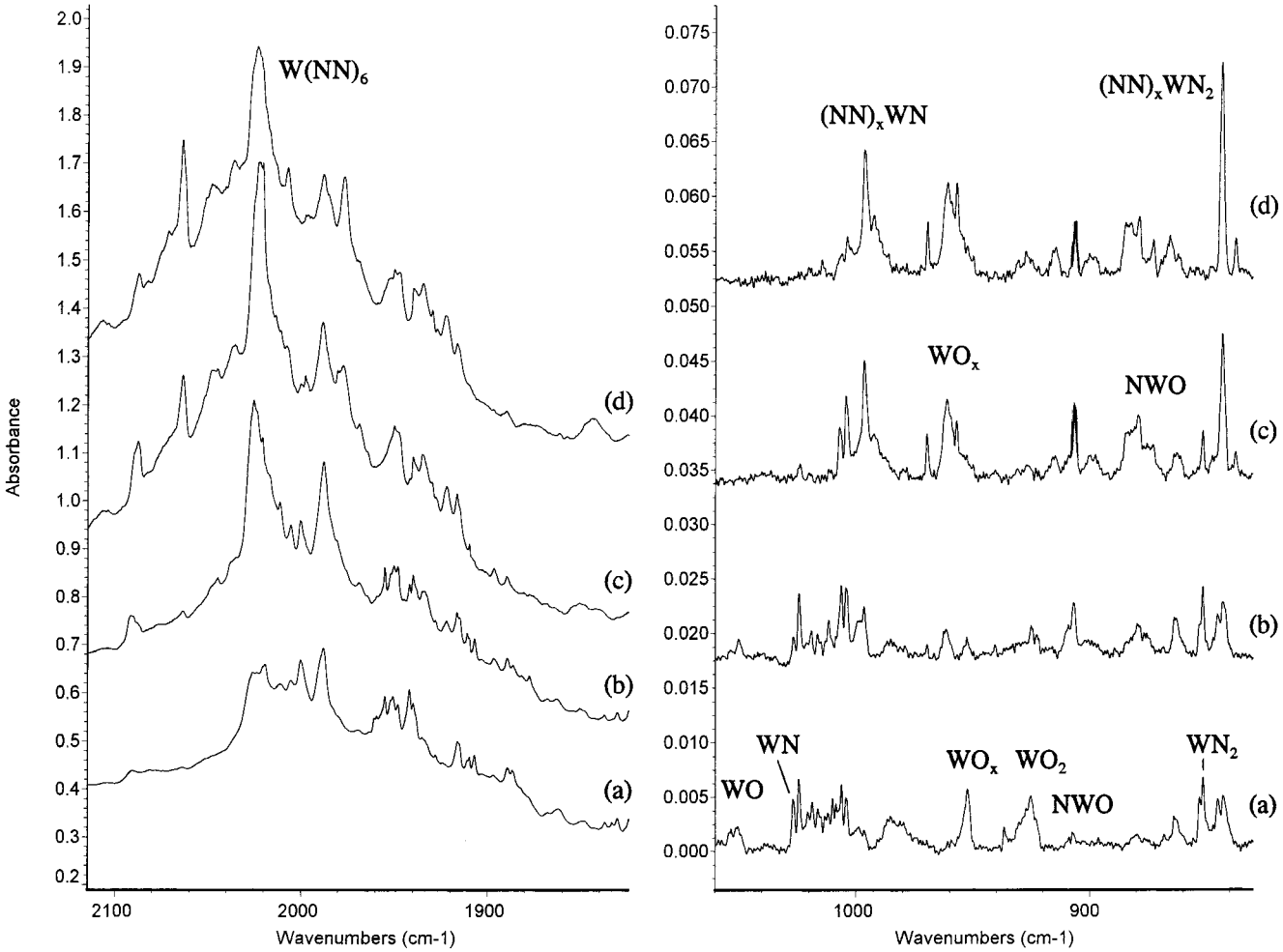

Figure 4. Infrared spectra in the 2115−1815 and 1060−830 cm^{-1} regions for laser-ablated W atoms codeposited with 4% $^{15}N_2$ in argon: (a) sample codeposited at 10 K for 2 h; (b) after annealing to 25 K; (c) after annealing to 30 K; (d) after annealing to 35 K; (e) after annealing to 40 K.

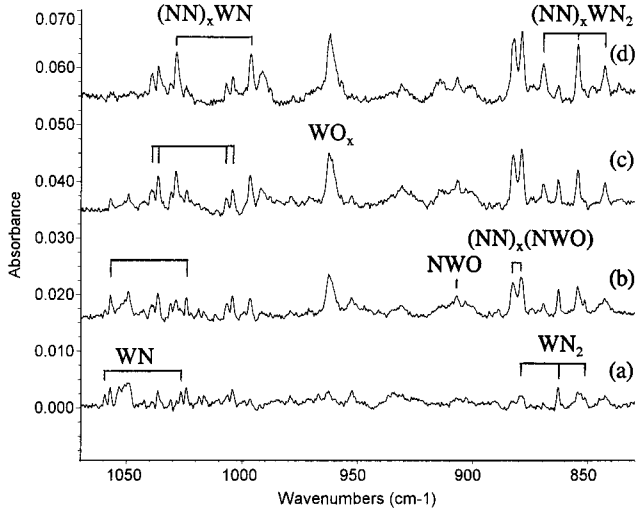

Figure 5. Infrared spectra in the 1070−830 cm^{-1} region for laser-ablated W atoms codeposited with 1% $^{14}N_2$ + 2% $^{14}N^{15}N$ + 1% $^{15}N_2$ in argon: (a) sample codeposited at 10 K for 75 min; (b) after annealing to 25 K; (c) after annealing to 30 K; (d) after annealing to 35 K; (e) after annealing to 40 K.

isotopic bands (1.03449) is indicative of a pure N−N stretching mode. The mixed isotopic antisymmetric N−N absorptions appear much like calculated spectra for the triply degenerate mode of octahedral complexes using isotopic mixtures.[59] The Mo and W spectra for both antisymmetric and symmetric modes for isotopic mixtures are similar to the matrix spectra for Cr(NN)$_6$ and Cr(CO)$_6$.[36,60] Accordingly, the above bands are assigned to octahedral Mo(NN)$_6$ and W(NN)$_6$, which is in accord with the octahedral structures for Mo(CO)$_6$ and W(CO)$_6$.[60−62] The four intermediate bands are then due to antisymmetric stretching modes in the M($^{14}N_2$)$_x$($^{15}N_2$)$_y$ ($x + y = 6$) complexes. Note that the 14/15 ratios for the highest/lowest upper bands observed for the symmetric modes of the mixed isotopic molecules (1.019, 1.020) are less than the pure N−N ratio. This is because the totally symmetric stretching modes for octahedral M($^{14}N_2$)$_6$ and M($^{15}N_2$)$_6$ are not allowed and the observed "intermediate" bands arise from lower symmetry isotopic molecules.

The bands at 520.5 and 523.0 cm^{-1} also give sextet absorptions, but the four intermediate mixed isotopic absorptions are stronger than the pure isotopic bands indicating different vibrational interaction between the M−NN and MN−N stretching modes. These lower absorptions contain a significant amount of M−NN stretching character based on the observation of ^{n}Mo isotopic structure for the analogous Mo(CO)$_6$ band at 600 cm^{-1}.[61]

The present 2113.9 cm^{-1} band is surely due to the same species absorbing at 2109.4 cm^{-1} in 95% N_2 + 5% Kr, which must be reassigned here to Mo(NN)$_6$. The intermediate mixed isotopic bands in the earlier study[20] are in accord with this reassignment.

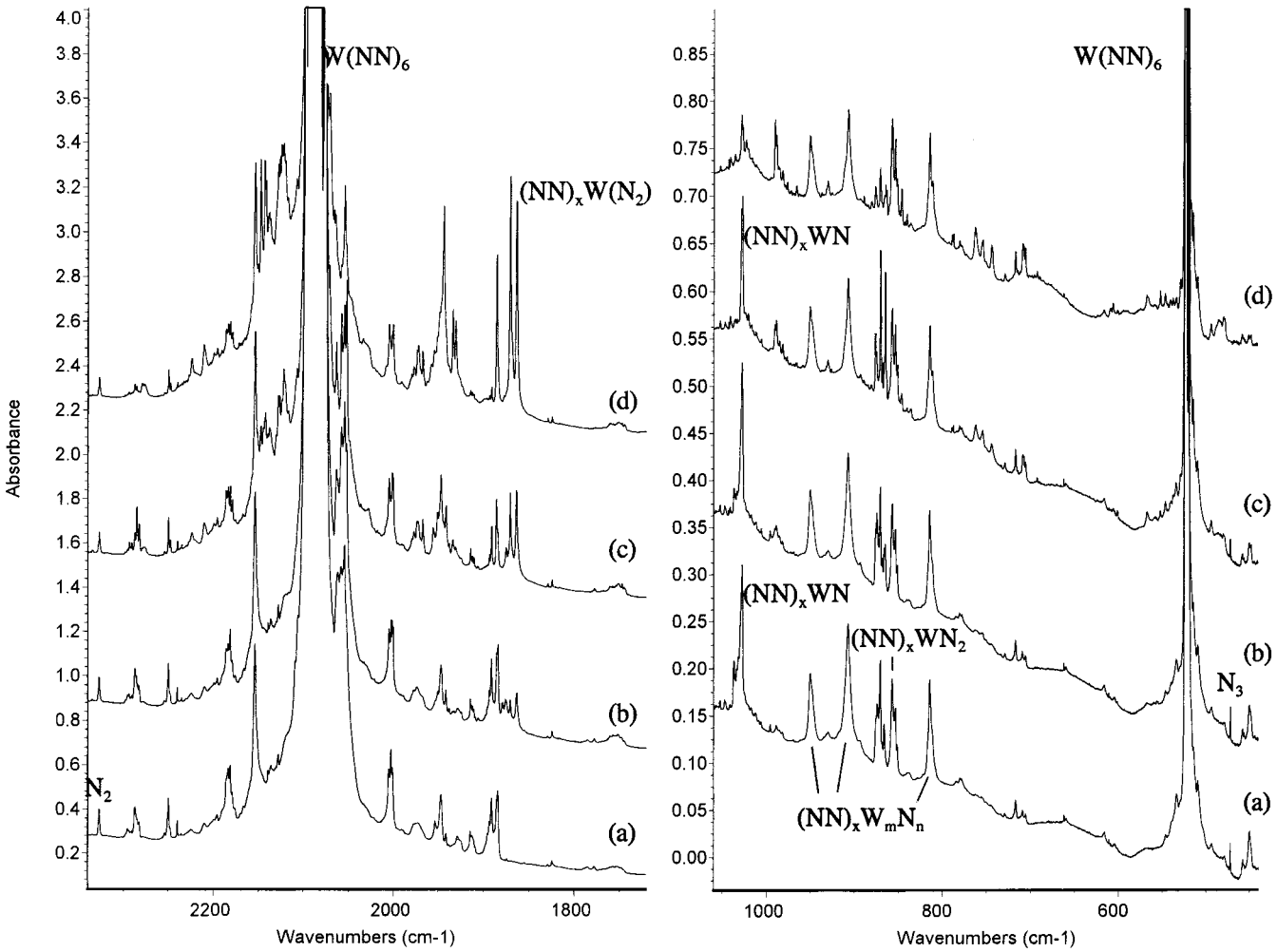

Figure 6. Infrared spectra in the 2340−1720 and 1060−440 cm^{-1} regions for laser-ablated W atoms codeposited with pure dinitrogen: (a) sample codeposited at 10 K for 1 h; (b) after annealing to 20 K; (c) after broadband photolysis for 20 min; (d) after annealing to 30 K; (e) after annealing to 35 K.

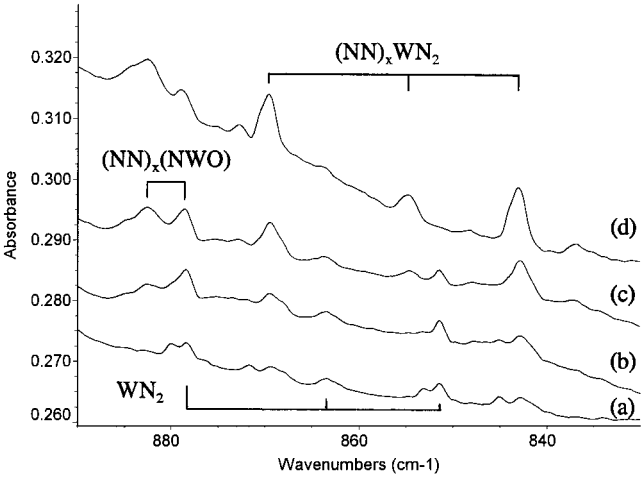

Figure 7. Infrared spectra in the 890−830 cm^{-1} region for laser-ablated W atoms codeposited with 2% $^{14}N_2$ + 2% $^{15}N_2$ in argon: (a) sample codeposited at 10 K for 90 min; (b) after annealing to 30 K; (c) after annealing to 35 K; (d) after annealing to 40 K.

The observation of $Mo(NN)_6$ and $W(NN)_6$ makes it likely that the monodinitrogen complexes are produced, but the identification of MoNN and WNN is not straightforward. The 2041.7 cm^{-1} band for Mo and 5% N_2 in solid krypton is probably due to a higher $Mo(NN)_x$ complex and not MoNN as first assigned. A better candidate is the sharp 1938.7 cm^{-1} band in solid argon, which decreases on annealing in favor of the broader 1964.8 cm^{-1} band, which increases then decreases on annealing in favor of higher frequency bands. The 2123.9 cm^{-1} argon matrix band may be due to $Mo(NN)_6$, observed at 2113.9 cm^{-1} in solid nitrogen, but we cannot be certain.

TABLE 6: Frequencies and Intensities Calculated (DFT/BP86) for Metal Nitrides and Dinitrides

molecule		structure	frequencies, cm^{-1} (intensities, km/mol)
MoN	$^4\Sigma^-$	1.657 Å	1090(72)
WN	$^4\Sigma^-$	1.678 Å	1089(32)
NMoN	$^1A_1$[a]	1.697 Å 104.2°	a_1, 1048(3); b_2, 933(283); a_1, 460(0)
	$^3B_2$[a]	1.721 Å 97.8°	a_1, 1006(63); b_2, 772(22); a_1, 350(1)
	$1A_1$[b]	1.684 Å 104.4°	a_1, 1025; b_2, 896; a_1, 461
	$^1A_1$[c]	1.68 Å 104.7°	a_1, 1078; b_2, 990; a_1, 469
NWN	$^1A_1$[d]	1.717 Å 104.3°	a_1, 1031(1); b_2, 964(30); a_1, 432(0)
	$^3B_2$[d]	1.731 Å 98.3°	a_1, 1024(21); b_2, 827(9); a_1, 341(3)
	$1A_1$[b]	1.707 Å 104.7°	a_1, 1025; b_2, 970; a_1, 431

[a] Dipole moments: $^1A_1$, 5.70 D; $^3B_2$, 3.89 D. [b] CCSD(T), ref 38. [c] LSDA, ref 37. [d] Dipole moments: $^1A_1$, 6.03 D; $^3B_2$, 4.45 D.

Four further observations support but cannot confirm assignment of the 1938.7 cm^{-1} band to MoNN. First, the band shows no intermediate component with $^{14}N_2 + {}^{15}N_2$. Second, DFT calculations predict $^5\Pi$ MoNN to absorb at 2003 cm^{-1}. Third, the pure dinitrogen experiments reveal weak bands in the low 1900 cm^{-1} region, which decrease on annealing and are destroyed by photolysis. Fourth, the analogous MoCO complex has been observed at 1862.6 cm^{-1}.[63]

Is there any evidence for sideways-bound $Mo(N_2)$? The bands at 1816.9 cm^{-1} show the appropriate isotopic behavior including a triplet with statistical $^{14,15}N_2$. This band increases slightly on first annealing and on photolysis, then decreases on higher temperature annealing. The 1816.9 cm^{-1} band is probably due to the complex $(NN)_xMo(N_2)$. This band is accompanied by a sharp 2149.5 cm^{-1} band for the end-bound ligand stretching mode, which shows the same band contour, annealing, and photolysis behavior. In addition, the sideways $^5B_1$ $Mo(N_2)$ complex is predicted by DFT to absorb at 1748 cm^{-1}, which is in the region of the present observations. Finally, the weak 1710.6 cm^{-1} band gives way on annealing, and this band could be due to $Mo(N_2)$, but more evidence is needed to support this interesting possibility.

The sharp 1894.3 cm^{-1} band with W and N_2 in argon parallels the 1938.7 cm^{-1} Mo feature, decreases on annealing, and is destroyed by photolysis. This band gives a doublet with $^{14}N_2 + {}^{15}N_2$ and is the best candidate for WNN. The analogous WCO species has been observed at 1848.8 cm^{-1}.[63] Stepwise annealing increases then decreases other features in the 2060−1950 cm^{-1} region, and the dominant band after annealing is at 2093 cm^{-1}. This strong absorption is probably due to $W(NN)_6$, based on similarity of the weaker intermediate mixed isotopic components with $^{14}N_2 + {}^{15}N_2$ in argon and the pure dinitrogen at 2087.7 cm^{-1} discussed above. Again, this is the mixed isotopic pattern expected for the triply degenerate mode of an octahedral complex.[59]

There is a relationship between the spectra for W and Mo in pure dinitrogen. The sharp 1871.0 and 1863.9 cm^{-1} bands appear on annealing, are destroyed by photolysis, and reappear on further annealing. These bands give a sharp doublet with $^{14}N_2 + {}^{15}N_2$, so the vibration of a single NN subunit is indicated. The weak 1747.3 cm^{-1} feature increased then decreased on stepwise annealing and formed a doublet with $^{14}N_2 + {}^{15}N_2$ with no evidence of secondary isotopic interactions. This W band is counterpart to the 1710.6 cm^{-1} Mo feature, and the 1747.3 cm^{-1} band could be due to sideways-bound $W(N_2)$, which acquires end-bound ligands on annealing and absorbs at 1871.0, 1863.9 cm^{-1}, although there is no evidence for the photolysis product. Sharp 2147.9, 2143.2 cm^{-1} bands exhibit the same photolysis and annealing behavior and are due to end-bound ligand vibrations of this $(NN)_xW(N_2)$ species. Absorptions between 2060 and 1880 cm^{-1} are weak and suggest that, in pure dinitrogen, reaction to give $W(NN)_6$ is extremely favorable.

Conclusions

Laser-ablated Mo and W atoms react with N_2 to form the metal nitride and dinitride molecules and their ligated N_2 complexes. The argon matrix fundamental of ^{98}MoN (1037.5 cm^{-1}) is in excellent agreement with the gas-phase value (1044.7 cm^{-1}), and accordingly the argon matrix fundamental for WN (1059.5 cm^{-1}) is an excellent predictor of the gas-phase WN frequency.

Following the observation of open, bent NCrN (956, 876 cm^{-1}), the NMoN (975, 860 cm^{-1}) and NWN (870 cm^{-1}) dinitride molecules have been characterized. Natural abundance Mo and ^{15}N substitution provide a 106 ± 3° determination of the N−Mo−N valence angle. Electronic structure calculations suggest the $^1A_1$ state for these bent dinitride molecules with some metal−nitrogen triple bond character. The observation of higher frequencies for W over Mo nitrides is due to the well-known relativistic contraction to compensate for shell expansion for third-row transition metals.[64] Finally, it is interesting to compare the linear NNdN (778 cm^{-1}) and NUN (1008, 1051 cm^{-1}) molecules, as Nd and U can be considered heavier members of group VI. Note that the inclusion of f orbitals changes the structure to linear, and shell expansion to Nd gives a lower frequency (and weaker bond), but this is reversed for U with the strong relativistic effect.[49,53,54]

Owing to the resolution of sharp $^{14}N_2 + {}^{15}N_2$ mixed isotopic absorptions that characterize the vibrations of octahedral symmetry, the octahedral $Mo(NN)_6$ and $W(NN)_6$ complexes have been identified by very strong 2113.9 and 2087.7 cm^{-1} and strong 520.5 and 523.0 cm^{-1} absorptions, respectively. Observation of the $M(NN)_6$ complexes suggests that the simple end-bonded complexes should be formed in these experiments. Although the identification is not ironclad, sharp, weak bands at 1938.7 and 1894.3 cm^{-1} are probably due to MoNN and WNN, respectively, in solid argon, which are 76 and 46 cm^{-1} higher than MoCO and WCO.[63] In solid nitrogen, the lowest frequency N−N stretching modes at 1710.6 and 1747.3 cm^{-1} could be due to the side-bound complexes $Mo(N_2)$ and $W(N_2)$, respectively, ligated with dinitrogen but this possible identification is tentative.

Although broad bands at 950, 906, and 814 cm^{-1} in the W/N_2 system are spectroscopically mundane, they are chemically interesting. The 14/15 shifts suggest the involvement of tungsten clusters and the mixed isotopic spectra require three or more nitrogen atoms. Similar features were observed at 935, 833, and 772 cm^{-1} in the Mo/N_2 system. Observation of these higher metal nitride clusters demonstrates the high reactivity of tungsten and molybdenum with nitrogen, as found in the gas phase.[57,58]

Acknowledgment. The authors gratefully acknowledge support from the Air Force Office of Scientific Research and consultation with A. Citra and M. F. Zhou.

References and Notes

(1) Chatt, J.; Dilworth, J. R.; Richards, R. L. *Chem. Rev.* **1978**, *78*, 589.
(2) Kim, J.; Rees, D. C. *Science* **1992**, *257*, 1677.
(3) Kim, J.; Rees, D. C. *Science* **1993**, *260*, 792.
(4) Crabtree, R. H. *The Organometallic Chemistry of the Transition Metals*, 2nd ed.; John Wiley and Sons: New York, 1994.
(5) Leigh, G. J. *Science* **1997**, *275*, 1442.
(6) Leigh, G. J. *Science* **1998**, *279*, 506.
(7) Cotton, F. A.; Wilkinson, G. *Advanced Inorganic Chemistry: A Comprehensive Text*, 5th ed.; Interscience Publishers: New York, 1988.
(8) Komori, K.; Oshita, H.; Mizobe, Y. *J. Am. Chem. Soc.* **1989**, *111*, 1939.
(9) Ishii, Y.; Ishino, Y.; Aoki, T.; Hiadi, M. *J. Am. Chem. Soc.* **1992**, *114*, 5429.
(10) Laplaza, C. E.; Cummins, C. C. *Science* **1997**, *268*, 861.
(11) Cui, Q.; Musaev, D.-G.; Svensson, M. *J. Am. Chem. Soc.* **1995**, *117*, 12366.
(12) Kim, M. J.; Brown, D. M.; Katz, W. *J. Electrochem. Soc.* **1983**, *130*, 1196.
(13) Huber, K. J.; Aita, C. R. *J. Vac. Sci. Technol. A* **1988**, *6*, 1717.
(14) Porowski, S.; Grzegory, I.; Morawski, A. *Mater. Processes* **1992**, *3*, 227.
(15) Kim, Y.-T.; Lee, C.-W. *J. Appl. Phys.* **1994**, *76*, 542.
(16) Ramanathan, S.; Oyama, S.-T. *J. Phys. Chem.* **1995**, *99*, 16365.
(17) Williams, W. S. *J. Metals* **1997**, *49*, 38.
(18) Rettner, C. T.; Stein, H.; Schweizer, E. K. *J. Chem. Phys.* **1988**, *89*, 3337.
(19) Lian, L.; Mitchell, S. A.; Rayner, D. M. *J. Phys. Chem.* **1994**, *98*, 11637.

(20) Foosnaes, T.; Pellin, M. J.; Gruen, D. M. *J. Chem. Phys.* **1983**, *78*, 2289.
(21) Fletcher, D. A.; Jung, K. Y.; Steimle, T. C. *J. Chem. Phys.* **1993**, *99*, 901.
(22) Jung, K. Y.; Fletcher, D. A.; Steimle, T. C. *J. Mol. Spectrosc.* **1994**, *165*, 448.
(23) Howard, J. C.; Conway, J. G. *J. Chem. Phys.* **1965**, *43*, 3055.
(24) Carlson, R. C.; Bates, J. K.; Dunn, T. M. *J. Mol. Spectrosc.* **1985**, *110*, 215.
(25) Allison, J. N.; Goddard, W. A., III *Chem. Phys.* **1983**, *81*, 263.
(26) Pazyuk, E. A.; Moskvitina, E. N.; Kuzyakov, Yu. Ya. *Spectrosc. Lett.* **1988**, *21*, 447.
(27) Berezin, A. B.; Dmitruk, S. A.; Kataev, D. J. *Opt. Spcetrosc.* **1990**, *68*, 310.
(28) Sze, N. S.-K.; Cheung, A. S.-C. *J. Quant. Spectrosc. Radiat. Transfer* **1994**, *52*, 145.
(29) Sze, N. S.-K.; Cheung, A. S.-C. *J. Mol. Spectrosc.* **1995**, *173*, 194.
(30) Bates, J. K.; Gruen, D. M. *J. Mol. Spectrosc.* **1979**, *78*, 284.
(31) Knight, L. B., Jr.; Steadman, J. *J. Chem. Phys.* **1982**, *76*, 3378.
(32) Ram, R. S.; Bernath, P. F. *J. Opt. Soc. Am. B* **1994**, *11*, 225.
(33) Johnson-Carr, J. A.; Zanetti, N. C.; Schrock, R. R. *J. Am. Chem. Soc.* **1996**, *118*, 11305. Schrock, R. R. *Acc. Chem. Res.* **1997**, *30*, 9.
(34) Harrison, J. F. *J. Phys. Chem.* **1996**, *100*, 3513.
(35) Balfour, W. J.; Qian, C. Z. W.; Zhou, C. *J. Chem. Phys.* **1997**, *106*, 4383; **1997**, *107*, 4473.
(36) Andrews, L.; Bare, W. D.; Chertihin, G. V. *J. Phys. Chem. A* **1997**, *101*, 8417.
(37) Martinez, A.; Köster, A. M.; Salahub, D. R. *J. Phys. Chem. A* **1997**, *101*, 1532.
(38) Pyykkö, P.; Tamm, T. *J. Phys. Chem. A* **1997**, *101*, 8107; Personal communication, 1999.
(39) Hassanzadeh, P.; Andrews, L. *J. Phys. Chem.* **1992**, *96*, 9177.
(40) Bare, W. D.; Souter, P. F.; Andrews, L. *J. Phys. Chem. A* **1998**, *102*, 8279.
(41) Frisch, M. J.; Trucks, G. W.; Schlegel, H. B.; Gill, P. M. W.; Johnson, B. G.; Robb, M. A.; Cheeseman, J. R.; Keith, T.; Petersson, G. A.; Montgomery, J. A.; Raghavachari, K.; Al-Laham, M. A.; Zakrzewski, V. G.; Ortiz, J. V.; Foresman, J. B.; Cioslowski, J.; Stefanov, B. B.; Nanayakkara, A.; Challacombe, M.; Peng, C. Y.; Ayala, P. Y.; Chen, W.; Wong, M. W.; Andres, J. L.; Replogle, E. S.; Gomperts, R.; Martin, R. L.; Fox, D. J.; Binkley, J. S.; Defrees, D. J.; Baker, J.; Stewart, J. P.; Head-Gordon, M.; Gonzalez, C.; Pople, J. A. *Gaussian 94*, revision B.1; Gaussian, Inc.: Pittsburgh, PA, 1995.
(42) Perdew, J. P. *Phys. Rev. B* **1986**, *33*, 8822. Becke, A. D. *J. Chem. Phys.* **1993**, *98*, 5648.
(43) Dunning, T. H., Jr.; Hay, P. J. In *Modern Theoretical Chemistry*; Schaefer, H. F., III, Ed.; Plenum: NewYork, 1976.
(44) Hay, P. J.; Wadt, W. R. *J. Chem. Phys.* **1985**, *82*, 299.
(45) Scott, A. P.; Radom, L. *J. Phys. Chem.* **1996**, *100*, 16502. Bytheway, I.; Wong, M. W. *Chem. Phys. Lett.* **1998**, *282*, 219.
(46) Allavena, M.; Rysnik, R.; White, D.; Calder, V.; Mann, D. E. *J. Chem. Phys.* **1969**, *50*, 3399.
(47) Andrews, L.; Zhou, M. F. *J. Phys. Chem. A*, in press (Mo, W + NO).
(48) Zhou, M. F.; Andrews, L. *J. Phys. Chem. A* **1998**, *102*, 9061.
(49) Willson, S. P.; Andrews, L. *J. Phys. Chem. A* **1998**, *102*, 10238.
(50) Andrews, L. *J. Electron Spectrosc. Relat. Phenom.* **1998**, *97*, 63.
(51) Kang, H.; Beauchamp, J. L. *J. Phys. Chem.* **1985**, *89*, 3364.
(52) Tiam, R.; Facelli, J. C.; Michl, J. *J. Phys. Chem.* **1988**, *92*, 4073.
(53) Hunt, R. D.; Yustein, J.; Andrews, L. *J. Chem. Phys.* **1993**, *98*, 6070.
(54) Pyykkö, P.; Li, J.; Runeberg, N. *J. Phys. Chem.* **1994**, *98*, 4809.
(55) Haaland, A.; Hammel, A.; Rypdal, K.; Volden, H. V. *J. Am. Chem. Soc.* **1990**, *112*, 4547.
(56) Kaupp, M. *J. Am. Chem. Soc.* **1996**, *118*, 3018.
(57) Mitchell, S. A.; Lian, L.; Rayner, D. M.; Hackett, P. A. *J. Chem. Phys.* **1995**, *103*, 5539.
(58) Mitchell, S. A.; Rayner, D. M.; Bartlett, T.; Hackett, P. A. *J. Chem. Phys.* **1996**, *104*, 4012.
(59) Darling, J. H.; Ogden, J. S. *J. Chem. Soc., Dalton Trans.* **1972**, 2496.
(60) Perutz, R. N.; Turner, J. J. *Inorg. Chem.* **1975**, *14*, 262.
(61) Tevault, D.; Nakamoto, K. *Inorg. Chem.* **1975**, *14*, 2371.
(62) Arnesen, S. P.; Seip, R. *Acta Chem. Scand.* **1966**, *20*, 2711.
(63) Souter, P. F.; Andrews, L. *J. Am. Chem. Soc.* **1997**, *119*, 7350.
(64) Pyykkö, P. *Chem. Rev.* **1988**, *88*, 563.